Infrared Spectra of Matrix Isolated Alkali Tetrafluoroaluminates, $AlkAlF_4(g)$

Reidar Huglen*, Sven J. Cyvin**, and Harald A. Øye

Institutt for uorganisk kjemi, Norges tekniske høgskole, Universitetet i Trondheim, Norway

Z. Naturforsch **34a**, 1118–1129 (1979); received June 18, 1979

The 1 : 1 adduct compounds which are the prevailing vapour species over equimolar mixtures of AlkF and AlF_3 (Alk = Li, Na, K, Rb and Cs) in the temperature range 450–750 °C have been isolated in argon and nitrogen matrices and examined by infrared spectroscopy. Seven frequencies which are assigned to matrix isolated alkali tetrafluoroaluminate molecules have been found for all systems investigated. Group theoretical analysis and subsequent normal coordinate computations of the reassigned frequencies confirm a structural model for the $AlkAlF_4$ molecules having the symmetry C_{2v}. However, the results from this analysis cannot be taken as a definite confirmation of a true bidentate structure for these molecules in the vapour phase. The alkali metal-fluorine bond is found to be rather weak, and the Al-F terminal bond is found to be stronger than the Al-F bridge bond. Qualitative relations between matrix as well as vibrational shifts and potential energy distribution are discussed.

Introduction

Several studies on the vapour phase above mixtures of $AlkX\text{-}MeX_n$, where Alk is an alkali metal, Me is a metal from another group in the periodical system, and X is halogen or oxygen, have been carried out in recent years [1]. The present paper is concerned with the infrared spectra of $AlkAlF_4$ gaseous molecules isolated in argon and nitrogen matrices. It was hoped that the use of two matrices might facilitate correction for matrix effects and give a better assignment of frequencies. In addition, observed matrix shifts between matrices might be helpful in attributing the different frequencies to the $AlkAlF_4$ molecules, and these matrix shifts might also give a basis for the estimation of gas-phase frequencies. Furthermore, the perturbing effect of different alkali atoms on the $AlkAlF_4$ molecules should be visualized in the matrix isolation experiments and provide valuable information to explain the interactions which take place between the composite fluorides in these complexes.

It seems to be generally agreed that the equimolar composition $NaF\text{-}AlF_3$ vaporizes congruently [2]. From mass spectrometric measurements [3, 4], the major vapour species present above heated samples of $NaF\text{-}AlF_3$ was found to be $NaAlF_4(g)$. The rest is mainly the dimer $(NaAlF_4)_2$, but Na_2AlF_5 and AlF_3 have also been suggested to exist in small amounts in the vapour phase [5]. Likewise, for the other alkali fluoride-aluminium fluoride systems the major vapour species has been shown to be $AlkAlF_4$ [5, 6]. The $NaGaF_4$ molecule has been found in the corresponding system $NaF\text{-}GaF_3$ [7], and the $AlkScF_4$ gaseous molecules are present in the $AlkF\text{-}ScF_3$ systems [5].

The structure of the $AlkAlF_4$ (Alk = Li, Na) molecules has been investigated by high-temperature infrared spectroscopy [8], high-temperature electron diffraction [9] and matrix isolation infrared studies [10]. However, the structural characterization of the $AlkAlF_4$ gaseous molecules has not been conclusively established.

Experimental

The matrix isolation apparatus was of conventional design with a deposition chamber connected to a furnace for producing high-temperature vapour species. The apparatus has been described in detail elsewhere [11]. The refrigerator system used was a CTi Cryodyne Cryocooler, Model 21, capable of maintaining an ultimate temperature of 10 K. The temperature on the cold station was determined using a Chromel-Gold (0.07 atomic% Fe) thermocouple. An Oxford Precision Temperature Controller provided digital reading of the temperature.

* Present address: Norsk Hydro a.s., Karmøy Fabrikker, N-4265 Håvik, Norway.

** Permanent address: Institutt for Fysikalsk Kjemi, Norges Tekniske Høgskole, Universitetet i Trondheim, N-7034 Trondheim-NTH, Norway.

Reprint requests to Prof. Harald A. Øye, Institutt for uorganisk kjemi, Norges tekniske høgskole, Universitetet i Trondheim, N-7034 Trondheim-NTH, Norway.

0340-4811 / 79 / 0900-1118 $ 01.00/0.

An O-ring sealed rotable flange facilitated turning the deposition window (CsI) by 90° to switch from deposition of matrices to recording of spectra. Graphite has been shown to be a suitable container material for fluorides, and the Knudsen effusion cells were made from Graph-I-Tite G (Carborundum Co., New York) with an effusion orifice diameter of 0.04 cm. The temperature near the cell was determined by a Chromel Alumel thermocouple connected to a Eurotherm proportional controller. The furnace could be used at temperatures up to 950 °C. A Balzers oil diffusion pump connected in series to a two-stage rotation pump enabled evacuation of the apparatus. Matrix gas was let into the system by means of a Balzers vacuum needle valve.

The chemicals used were the following: LiF (Analyzed reagent, Baker), NaF, KF, RbF (p.a., Merck), CsF (99.9%, Schuchardt), AlF_3 (99.0%, Riedel de Häen, AG), and Ar and N_2 (99.997%, Norsk Hydro a.s.).

The alkalifluorides were dried under vacuum, melted and purified by recrystallization. AlF_3 was sublimed twice in a vacuum furnace at about 900 °C. Argon and nitrogen were used without purification.

Before starting matrix deposition, the vacuum chamber was evacuated to $5 \cdot 10^{-6}$ torr. Deposition times for the matrices varied from two to five hours. During deposition, the temperature remained constant at 13 ± 1.5 K. For a typical experiment matrix ratios were estimated to be in the range 800—5000 [11]. Spectra were recorded on a Perkin Elmer 457 spectrophotometer. Reported frequencies are accurate within ± 2 cm^{-1}.

Results

The infrared spectrum of the vapour above an equimolar mixture of AlkF (Alk = K) and AlF_3 isolated in argon matrices are presented in Fig. 1, whereas the nitrogen-isolated vapours (Alk = Li, Na, Cs) are shown in Figs. 2, 3 and 4. In Fig. 5 the region 650—600 cm^{-1} is shown in an expanded scale for the vapours (Alk = Li, Na, K, Rb and Cs) isolated in argon matrices.

The band positions were determined from three to seven different matrix isolation experiments, and the determined vibrational frequencies for the vapours isolated in argon matrices are listed in Table 1. The NaF-AlF_3 system was studied most extensively. The standard deviations in the band

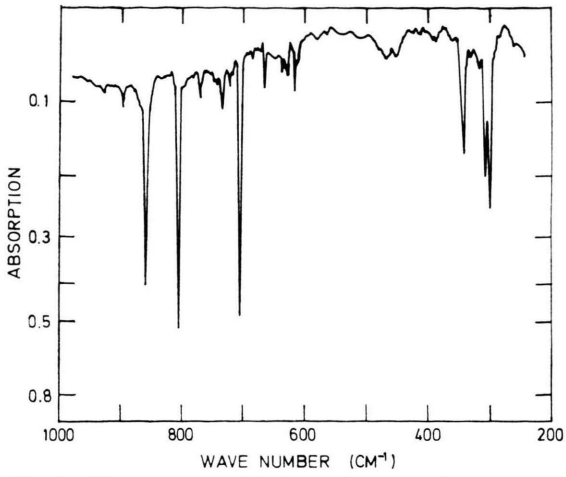

Fig. 1. IR spectrum of the vapour species above an equimolar mixture of KF-AlF_3 isolated in argon matrix. Deposition time, $4\frac{1}{2}$ hours at 600 °C.

Table 1. Characteristic frequencies (cm^{-1}) of vapour species above AlkF-AlF_3 isolated in argon matrices. Frequencies that have similar counterparts in all spectra and are attributed to $AlkAlF_4$ molecules, are given in italics. Intensities are given in parenthesis.

LiF-AlF_3	NaF-AlF_3	KF-AlF_3	RbF-AlF_3	CsF-AlF_3
945 (m)				
933 (m)				874 (m)
891 (s)	*877* (s)	*859* (s)	*858* (s)	*854* (s)
883 (w)	863 (m)			825 (vw)
	858 (s)			808 (w)
836 (w)			804 (s)	802 (w)
817 (s)	*808* (s)	*805* (s)	*801* (s)	*798* (s)
808 (w)				
797 (w)			788 (vw)	
			783 (vw)	
772 (w)		770 (vw)	771 (vw)	
			764 (vw)	
			744 (m)	748 (m)
			741 (m)	745 (m)
				739 (vw)
	736 (vw)	734 (vw)	736 (vw)	735 (vw)
722 (w)	721 (vw)	722 (vw)	722 (w)	722 (vw)
	715 (vw)		711 (s)	716 (vw)
652 (s)	*684* (s)	*705* (s)	*706* (s)	*709* (s)
	676 (m)			
669 (w)		669 (vw)	669 (vw)	669 (vw)
663 (w)	663 (w)	663 (w)	663 (w)	663 (w)
636 (vw)	636 (vw)	636 (vw)	636 (vw)	636 (vw)
630 (vw)	630 (vw)	630 (vw)	630 (vw)	630 (vw)
616 (w)	*619* (w)	*626* (w)	*624* (w)	*623* (w)
614 (w)	614 (w)	615 (w)	615 (w)	615 (w)
	391 (m)			
387 (m)	386 (m/w)sh			
517 (m/s)	*364* (m/s)	*343* (m/s)	*334* (m/s)	*326* (m/s)
337 (vw)				
330 (vw)		330 (vw)		
		318 (vw)		
409 (m/s)	*316* (m/s)	*308* (m/s)	*307* (m/s)	*305* (m/s)
310 (m/s)	*300* (m/s)	*301* (m/s)	*301* (m/s)	*301* (m/s)

s: strong, m: medium, w: weak, vw: very weak, sh: shoulder.

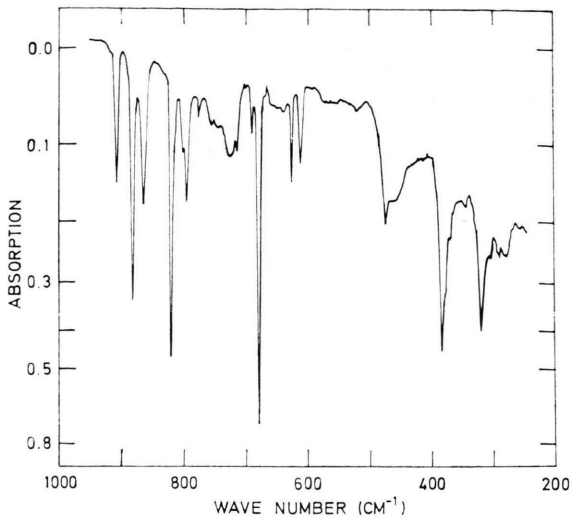

Fig. 2. IR spectrum of the vapour species above an equimolar mixture of $LiF\text{-}AlF_3$ isolated in nitrogen matrix. Deposition time, $2\frac{1}{2}$ hours at 700 °C.

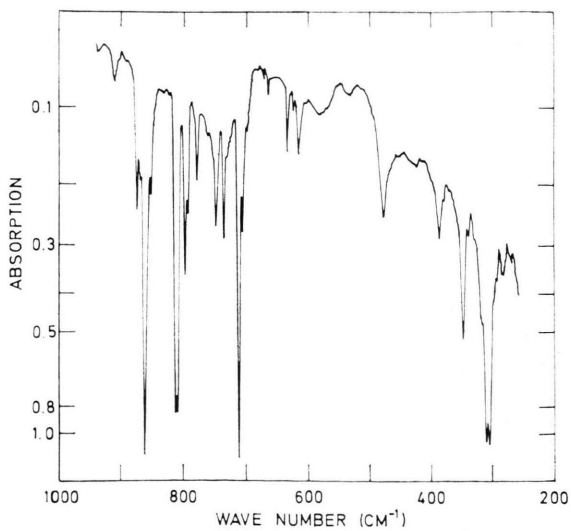

Fig. 3. IR spectrum of the vapour species above an equimolar mixture of $NaF\text{-}AlF_3$ isolated in nitrogen matrix. Deposition time, 4 hours at 655 °C.

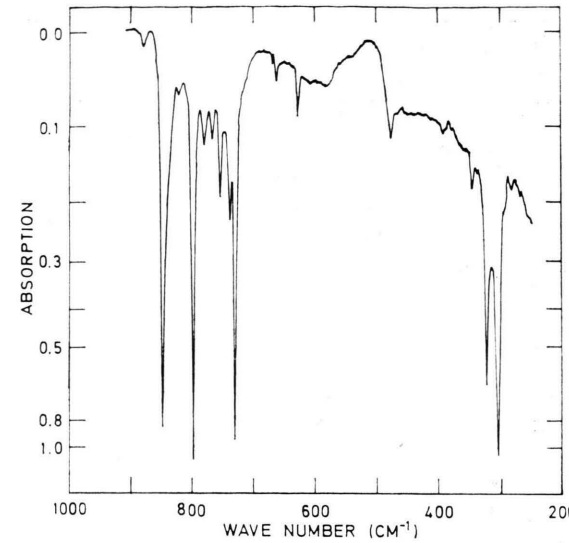

Fig. 4. IR spectrum of the vapour species above an equimolar mixture of $CsF\text{-}AlF_3$ isolated in nitrogen matrix. Deposition time, 3 hours at 485 °C.

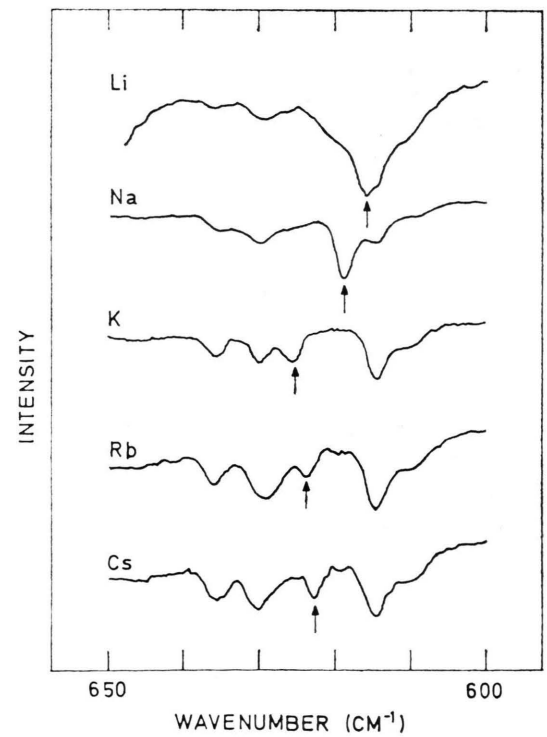

Fig. 5. The region 650–600 cm^{-1} expanded horizontally. The band which changes position when the alkali atom is exchanged, is marked with an arrow.

positions were found to be less than 1 cm^{-1} for all bands.

After prolonged deposition the matrices occasionally became opaque and non-transparent to visible light. However, this phenomenon did not have any significant influence on the recorded infrared spectra. For the AlkF-AlF_3 systems, evaporation was carried out in the temperature range 450—780 °C. As far as the occurrence of new absorption bands and significant changes in band intensities are concerned, the recorded spectra of the different systems did not depend on the evaporation temperature within the limits given above. No spectral evidence of AlF_3 and AlkF was found.

Assignment of Frequencies

The complexity of the spectra shown in Figs. 1—4 suggests that not all these frequencies can be assigned to the $AlkAlF_4$ molecules. The strong absorption bands may reasonably well be attributed to these vapour species. The weaker absorption bands may be assigned to the $AlkAlF_4$ molecules, to the dimers $Alk_2Al_2F_8$ or the complexes Alk_2AlF_5, even though the possibility cannot be ruled out that these absorptions may result from matrix effects and/or impurities from air leaks and outgassing of the furnace. In order to find the frequencies due to the $NaAlF_4$ molecule, a relative absorption band intensity ratio analysis has been carried out [12, 10]. Relative intensity ratios, with respect to the 877 cm^{-1} band (which is one of the strongest bands), were determined for the frequencies from four different spectra and are presented in Table 2.

Based on the calculated standard deviations shown in Table 2, the following frequencies, which have the lowest standard deviations, were chosen for further assignment: 877, 863, 858, 808, 684, 676, 619, 364, 316 and 300 cm^{-1}. The standard deviation of the 316 cm^{-1} absorption band intensity ratio is 34%, but it is included for further evaluation because of the strong and sharp absorption feature.

It is evident that relative intensity ratios are not reliable as a single criterion in assigning frequencies belonging to the $NaAlF_4$ molecule. This is at variance with the procedure used by Cyvin et al. [10], who assigned absorption bands to to the same species when the standard deviation of a set of relative intensity ratios was within ±7%. However, it seems obvious that there is a considerable error in their calculated standard deviations. The actual standard deviations seem clearly to be about three times higher than those published.

Table 2. Relative intensity measurements for the characteristic absorption bands in the spectrum of the vapour species above NaF-AlF_3 isolated in argon matrices. Frequencies chosen for further assignment are given in italics.

Characteristic frequency (cm^{-1})	$I_{877} : I$ Run number 4	5	6	7	Standard deviation ±%
877	1.00	1.00	1.00	1.00	
863	2.6	2.6	3.0	1.7	22.4
858	1.6	1.5	1.4	1.4	7.4
808	0.65	0.65	0.43	0.70	19.7
736	3.3	7.6	12.6	2.9	68.6
721	4.3	7.9	3.7	4.0	39.6
715	4.1	9.2	5.3	4.3	41.5
684	0.81	0.77	0.66	0.67	9.6
676	1.9	2.7	2.1	2.6	17.2
663	4.3	5.5	2.3	8.7	51.5
636	8.7	27.5	6.3	8.7	77.1
630	8.7	12.5	4.2	4.7	51.5
619	5.2	5.3	5.7	4.9	6.3
614	8.7	12.5	4.8	2.2	64.0
391	2.4	2.8	3.0	6.5	51.6
386	2.6	4.6		6.5	42.7
364	1.3	1.9	1.4	1.6	16.8
316	1.0	2.0	1.1	1.6	34.0
300	1.0	1.4	1.5	1.4	18.2
Furnace temperature, °C	645	675	665	650	

To make a more reliable assignment of frequencies, the above chosen absorption bands are compared with the characteristic frequencies for all $AlkAlF_4$ molecules isolated in argon matrices listed in Table 1. One would expect that the absorption bands belonging to the $AlkAlF_4$ molecules should be found in all spectra only with a small change in frequencies due to the influence of different alkali atoms. Indeed, Table 1 shows that the 877, 808, 684, 619, 364, 316 and 300 cm^{-1} absorption bands of the NaF-AlF_3 infrared spectrum have seven similar counterparts in the other AlkF-AlF_3 infrared spectra, and hence are attributed to the $NaAlF_4$ molecule isolated in an argon matrix. The 863, 858 and 676 cm^{-1} absorption bands do not have corresponding bands in the four other spectra. In Table 3 the frequencies related to the $AlkAlF_4$ molecules are listed.

A similar examination of the frequencies recorded for species isolated in nitrogen matrices shows that

Table 3. Infrared absorption band frequencies (cm^{-1}) assigned to $AlkAlF_4$ molecules (Alk = Li, Na, K, Rb, Cs) isolated in argon and nitrogen matrices. Values for $^6LiAlF_4$, $^7LiAlF_4$ and $NaAlF_4$ isolated in noen matrices are taken from Cyvin et al. [10].

Matrix	Neon			Argon					Nitrogen				
Alkali atom	^{6}Li	^{7}Li	Na	Li	Na	K	Rb	Cs	Li	Na	K	Rb	Cs
	901	900	884	891	877	859	858	854	883	861	850	850	849
	818	817	811	817	808	805	801	798	822	812	806	803	798
	651	649	674	652	684	705	706	709	680	711	721	726	730
	611*	611*	616*	616	619	626	624	623	628	631	629	630	630
			379										
	577	541	372	517	364	343	334	326	(477)	348	333	325	323
	453	433	323	409	316	308	307	305	(378)	310	308	305	304
	316	313	302	310	300	301	301	301	322	304	304	305	304
	269	268											
	222	221											

Frequencies in parenthesis are assumed to belong to the $AlkAlF_4$ molecule.

* Observed, but not assigned to the $AlkAlF_4$ molecules [10].

seven counterpart frequencies have been found in the spectra of $LiAlF_4$, $NaAlF_4$ and $KAlF_4$, while for $RbAlF_4$ and $CsAlF_4$ only six have been found. These frequencies may be assigned to the $AlkAlF_4$ molecules and are given in Table 3. However, the strong absorption band observed at 305 and 304 cm^{-1} for $RbAlF_4$ and $CsAlF_4$, respectively, is interpreted as being composed of two fundamentals not resolved by the spectrophotometer. Thus, seven fundamentals are also observed for these two molecules. Also in Table 3 the absorption frequencies reported by Cyvin et al. [10] for $^6LiAlF_4$, $^7LiAlF_4$ and $NaAlF_4$ in neon matrices are listed for comparison.

The observed spectra of matrix isolated $AlkAlF_4$ agree very well with the previous investigation of Cyvin et al. [10]. The most important discrepancy (as will be discussed below) between the spectra observed in this work and those previously reported appears in the present assignment to the $AlkAlF_4$ molecules of the weak absorption bands in the 610—630 cm^{-1} range. Based on their criterion for the relative intensity measurements, Cyvin et al. [10] were not able to attribute any absorption feature in this region to the $AlkAlF_4$ molecules investigated. However, they detected two absorption bands in the spectra of $LiAlF_4$ and $NaAlF_4$ in the actual region at 611, and 616 cm^{-1}, respectively. The frequencies at 611 and 616 cm^{-1} are assumed to correspond to the frequencies in the 610—630 cm^{-1} region assigned to the $AlkAlF_4$ molecules in this work (cf. Figure 5). This assumption is based on the reasonable frequency shift of 5 cm^{-1} when Li is substituted with Na.

The relatively strong absorption band at 379 cm^{-1} assigned to $NaAlF_4$ in a neon matrix, is neither found in argon and nitrogen matrices for $NaAlF_4$, nor does it have any counterpart frequencies in the spectra of the other matrix isolated $AlkAlF_4$ molecules. Most probably it is the result of matrix splitting of a single fundamental frequency (379 to 372 cm^{-1}). Splittings of similar order of magnitudes have been observed for $NaAlF_4$ and $RbAlF_4$ in argon matrices (at 684—676 cm^{-1} and 711 to 706 cm^{-1}, respectively). Likewise such splitting patterns have been observed for Li_2F_2 [13], $LiNaF_2$ [12] and also for $^6LiAlF_4$ and $^7LiAlF_4$ [10].

The two lowest frequencies found for $^6LiAlF_4$ and $^7LiAlF_4$ in neon matrices at about 270 and 220 cm^{-1} were not discovered with $LiAlF_4$ trapped in argon and nitrogen matrices. This may be explained by the fact that the spectrophotometric limit of the infrared instrument used in this work is 250 cm^{-1}, indicating that the energetic conditions and the resolution of the last 50 cm^{-1} are not as good as in the higher frequency range.

Molecular Models

Three structural models involving tetrahedral AlF_4 can be postulated for the $AlkAlF_4$ molecules as shown in Figure 6. The alkali atom may be attached to one fluorine, or shared by two or three fluorine atoms, respectively. Models I and III with

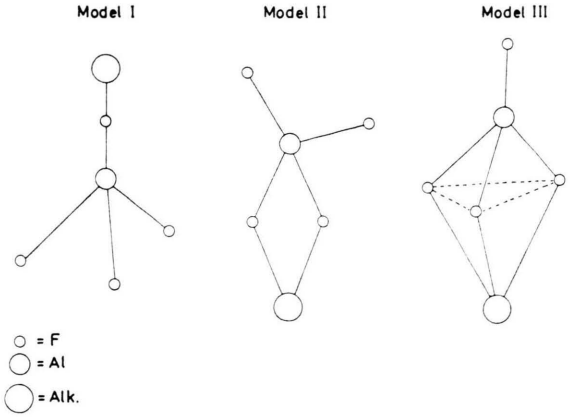

Fig. 6. Three possible structural models for $AlkAlF_4$.

C_{3v}-symmetry should give 8 frequencies active in the infrared and Raman, while the C_{2v}-model (Model II) has 12 Raman active fundamentals and 11 active in the infrared. Porter and Zeller [6] proposed Model III, while results from high-temperature diffraction [9] and IR-studies [10] were interpreted in favour of a structure having symmetry C_{2v} (Model II). The preference of Model II rather than Model III has been discussed on the basis of existing spectral and thermodynamic evidence [14]. Due to the occurence of inconsistencies in a preliminary normal coordinate analysis for Models I and II, no preference could be given to one of the two models in describing the molecular geometry [15]. However, this analysis was performed before the weak absorption bands between 610 to 630 cm^{-1} were assigned to the $AlkAlF_4$ molecules.

Structural data from gas electron diffraction are available for $KAlCl_4$ [16], $KYCl_4$ [17], $TlInCl_4$ [18] and the two structurally related molecules with oxygen bridges: $KReO_4$ [19] and $TlReO_4$ [20]. The most probable symmetrical structure deduced for all these molecules is represented by Model II. $LiBeF_3$ trapped in neon matrix has also been reported to have C_{2v}-symmetry [21].

The Raman spectrum of molten $AlkF\text{-}AlF_3$ has been reported proving the existence of the AlF_4^- anion with T_d symmetry [22]. The stretching frequencies were found at $\nu_1(A_1) = 622\ cm^{-1}$ and $\nu_3(F_2) = 760\ cm^{-1}$, and the bending frequencies at $\nu_2(E) = 210\ cm^{-1}$ and $\nu_4(F_2) = 322\ cm^{-1}$. Others have also reported on the totally symmetric stretching frequency of a tetrahedral AlF_4^- ion [23—25].

Lowering the symmetry from T_d to C_{3v} makes the triple degenerate fundamental $T_d(F_2)$ to split into two fundamentals $C_{3v}(A_1 + E)$, and lowering the symmetry to C_{2v} removes the degeneracy to three fundamentals $C_{2v}(A_1 + B_1 + B_2)$. Normally, the $AlkAlF_4$ molecule should then have three Al-F stretching vibrations in the region 600—900 cm^{-1} if the molecular symmetry is C_{3v}, and have four vibrations in this stretching region if the symmetry is reduced to C_{2v}. Since the totally symmetric stretching frequency $\nu_1(A_1)$ is infrared inactive in the T_d symmetry, this fundamental is expected to have low intensity in the perturbed $AlkAlF_4$ molecule.

The C_{2v} model then provides a straightforward explanation of the observed frequencies (> 600 cm^{-1}) listed in Table 3. For all the molecules, three frequencies of comparable intensities have been observed in the range 650—900 cm^{-1}, while a weak absorption band is seen in all spectra between 610—630 cm^{-1} (cf. Figure 5). These results are in good agreement with the frequency assignment given for the matrix isolated alkali metal perchlorate ion pairs, $Alk^+ClO_4^-$, which were interpreted to have a bidentate C_{2v} symmetry [26].

In order to establish a sound basis for force constant approximations in the normal coordinate analysis, approximate force constants for AlF_4^- with T_d symmetry were calculated using the L-matrix method [27, 28] and a simple Urey-Bradley-Shimanouchi (UBS) force field approximation [29, 30], Table 4. The valence force constands f_α and $f_{\alpha\alpha}$ were calculated from the assumption $f_{\alpha\alpha'} = 0$.

Normal Coordinate Analysis

The normal coordinate analysis for the $AlkAlF_4$ molecules are based on the molecular Model II of Fig. 6 with C_{2v} symmetry. The complete set of symmetry coordinates without redundants have been described elsewhere [10, 11].

The following types of valence coordinates were employed: s(Alk-F), r(Al-F_b), d(Al-F_t) stretchings, $\alpha(F_bAlF_b)$, β(AlFAlk), $\gamma(F_bAlkF_b)$, $\delta(F_tAlF_t)$, $\varphi(F_tAlF_b)$ bendings (b: bridge, t: terminal, and w: ring deformation). The symmetry coordinates are distributed according to the representation:

$$\Gamma(Q) = 5A_1 + A_2 + 3B_1 + 3B_2 .$$

All of the Al-F_b and Al-F_t bonds were assumed to be 1.69 Å in accordance with the gas electron diffraction results for $NaAlF_4$ [9]. The following Alk-F bond lengths (in Å) were adopted: Cs: 2.50, Rb: 2.40, K: 2.30 (approximated values), Na: 2.11, and Li: 1.68 [10]. The F_tAlF_t angle in Model II, Fig. 6, as well as all FAlF angles in Models I and III, were assumed to be tetrahedral. The F_bAlF_b angle for Model II with all alkali atoms was taken as 110° [10]. Some possible inaccuracies in the structural parameters are assumed to have a relatively minor influence on the normal coordinate analysis.

On the basis of the force constant calculations for the tetrahedral AlF_4^- ion, and the previously reported force fields for $LiAlF_4$ and $NaAlF_4$ [10], simple force fields were approximated.

Six bending force constants (f_α, f_δ and f_φ) of 0.3 mdyne/Å (cf. Table 4) were used for all molecules. The f_β, f_γ and f_w force constants were maintained at 0.1 mdyne/Å for all compounds, irrespectively of the alkali atom. The f_s force constant is assumed to increase from CsF to LiF. When introducing the alkali atom to the AlF_4^- tetrahedron, the f_r force constant is assumed to become weaker than the f_d force constant. Furthermore, f_r is supposed to decrease and f_d to increase when the alkali atom is changed from Cs to Li. Table 5 shows the variation of the initial stretching force constants with different alkali atoms.

These initial approximate force fields are based on valence coordinates including redundancies and are represented by a diagonal matrix with the elements f_d, f_r, f_s, f_α, f_φ, f_δ, f_w, f_β and f_γ. The valence force field matrix was transformed to the symmetry F matrix by means of the T matrix techniques [31, 32, 33].

Table 4. Symmetry and valence force constants (mdyne/Å) of tetrahedral AlF_4^-. Frequencies used: $\nu_1 = 622$, $\nu_3 = 760$, $\nu_2 = 210$, and $\nu_4 = 322$ cm^{-1} [23].

Force constant	UBS-method	L-matrix method
$F_{11}(A_1)$	4.33	4.33
$F_{11}(E)$	0.16	0.16
$F_{11}(F_2)$	3.32	3.61
$F_{12}(F_2)$	−0.15	−0.29
$F_{22}(F_2)$	0.30	0.29
f_r	3.57	3.79
f_{rr}	0.25	0.18
$f_{r\alpha} - f_{r\alpha}$	0.10	0.20
f_α	0.30	0.29
$f_{\alpha\alpha}$	0.07	0.07

Table 5. Approximate stretching force constants (mdyne/Å) for $AlkAlF_4$ used in the initial force field calculation.

	Cs	Rb	K	Na	Li
f_s (Alk-F)	0.15	0.18	0.25	0.38	0.60
f_r (Al-F_b)	3.70	3.65	3.55	3.40	3.20
f_d (Al-F_t)	4.00	4.05	4.15	4.30	4.50

The connection between the symmetry force constants of the F-matrix and the valence force constants of the $\hat{F}$-matrix is difficult to survey, and have therefore been developed explicitly [11]. In addition to the diagonal constants the four interaction constants f_{dd}, f_{rr}, f_{rd} and f_{ss} were included in the $\hat{F}$-matrix. The coefficients relating the two kinds of force constants are shown in Table 6 where structural parameters for $CsAlF_4$ are used.

Working out from the initial force fields of Table 4, a set of approximate valence force constants were obtained (Table 7) that gave a good fit between observed and calculated frequencies.

Table 6. Symmetry force constants for $CsAlF_4$ (C_{2v}-symmetry) expressed numerically in terms of valence force constants. Structural parameters are taken from the information given in the text.

Species A_1	$F_{11} = f_r + f_{rr} + 0.65 f_\beta + 1.93 f_\gamma$
	$F_{12} = -0.44 f_\beta - 1.31 f_\gamma$
	$F_{14} = 1.17 f_\beta + 0.96 f_\gamma$
	$F_{22} = f_s + f_{ss} + 0.30 f_\beta + 0.88 f_\gamma$
	$F_{24} = -0.69 f_\beta - 0.65 f_\gamma$
	$F_{44} = f_\alpha + 1.59 f_\beta + 0.48 f_\gamma + 1.02 f_\delta$
	$F_{45} = 2.02 f_\delta$
	$F_{55} = f_\varphi + 4.00 f_\delta$
Species B_2	$F_{11} = f_r - f_{rr} + 0.73 f_\beta$
	$F_{12} = 1.05 f_\beta$
	$F_{22} = f_s - f_{ss} + 1.53 f_\beta$

Table 7. Approximate valence force constants (mdyne/Å) for $AlkAlF_4$ molecules with symmetry C_{2v}.

Valence force constants	$CsAlF_4$	$RbAlF_4$	$KAlF_4$	$NaAlF_4$	$LiAlF_4$
f_d (Al-F_t)	4.20	4.25	4.30	4.45	4.60
f_{dd}	0.20	0.20	0.20	0.25	0.25
f_r (Al-F_b)	2.85	2.80	2.80	2.65	2.40
f_{rr}	0.35	0.35	0.35	0.35	0.40
f_{rd}	0.30	0.30	0.30	0.30	0.30
f_s (Alk-F)	0.15	0.18	0.25	0.36	0.66
f_{ss}	0.00	0.00	0.00	0.02	0.20
f_α (F_b-Al-F_b)	0.28	0.30	0.30	0.30	0.30
f_φ (F_t-Al-F_b)	0.27	0.27	0.27	0.27	0.27
f_δ (F_t-Al-F_t)	0.27	0.27	0.27	0.27	0.27
f_w (ring def.)	0.09	0.09	0.09	0.09	0.10
f_β (Al-F_b-Alk)	0.05	0.05	0.05	0.05	0.10
f_γ (F_b-Alk-F_b)	0.05	0.05	0.05	0.05	0.13

The introduction of interaction constants, e.g. f_{rr}, f_{dd} and f_{rd}, and the increase of f_d and decrease of f_r, satisfactorily account for the observed variation of the Al-F stretching frequencies. However, introduction of the f_{ss} interaction constant forces the highest ν_4 frequency of $LiAlF_4$ into A_1 from B_2.

The calculated frequencies from these approximate force fields are shown in Table 8 together with a tentative assignment for the observed frequencies of Table 3. The inactive one-dimensional A_2 species is omitted.

Table 8. Tentative assignment for the observed and calculated frequencies (cm^{-1}) of the $AlkAlF_4$ molecules with C_{2v}-symmetry. Potential energy distributions (PED) are also given. The valence coordinates d, r, s, α and φ correspond to the valence force constants of Table 7.

Species	Calculated		Obs.[a]	PED[b]
	approx.	final		
		$CsAlF_4$		
A_1 (ν_{3b})	795	798	798	$0.82d + 0.24r + 0.11\alpha$
(ν_1)	613	620	620	$0.73r + 0.15d$
(ν_{4a})	329	330	330	$1.34\alpha + 0.21\varphi$
	279	280	unobs.	1.26φ
	90	90	unobs. (<250)	0.91s
B_1 (ν_{3a})	864	868	868	0.91d
(ν_{4c})	318	303	303	$0.80\varphi + 0.15w$
	76	76	unobs. (<250)	$0.85w + 0.13\varphi$
B_2 (ν_{3c})	704	699	699	$0.88r + 0.15\varphi$
(ν_{4b})	295	308	308	$0.81\varphi + 0.12r$
	136	136	unobs. (<250)	0.96s
		$RbAlF_4$		
A_1 (ν_{3b})	799	801	801	$0.83d + 0.23r + 0.11\alpha$
(ν_1)	611	619	619	$0.75r + 0.14d$
(ν_{4a})	337	341	341	$1.31\alpha + 0.24\varphi + 0.12s$
	281	281	unobs.	1.17φ
	106	106	unobs. (<250)	0.88s
B_1 (ν_{3a})	869	874	874	0.91d
(ν_{4c})	318	303	303	$0.80\varphi + 0.15w$
	79	79	unobs. (<250)	$0.85w + 0.13\varphi$
B_2 (ν_{3c})	698	696	696	$0.87r + 0.15\varphi$
(ν_{4b})	295	312	312	$0.80\varphi + 0.13r$
	148	148	unobs. (<250)	0.96s
		$KAlF_4$		
A_1 (ν_{3b})	803	805	805	$0.83d + 0.22r + 0.11\alpha$
(ν_1)	611	618	618	$0.76r + 0.14d$
(ν_{4a})	344	351	351	$1.27\alpha + 0.28\varphi + 0.20s$
	283	284	unobs.	1.03φ
	150	149	unobs. (<250)	$0.78s + 0.18\varphi + 0.12\alpha$
B_1 (ν_{3a})	874	877	877	0.91d
(ν_{4c})	319	303	303	$0.80\varphi + 0.16w$
	90	90	unobs. (<250)	$0.84w + 0.14\varphi$
B_2 (ν_{3c})	698	695	695	$0.88r + 0.15\varphi$
(ν_{4b})	297	317	317	$0.76\varphi + 0.13r$
	182	175	unobs. (<250)	0.93s
		$NaAlF_4$		
A_1 (ν_{3b})	815	808	808	$0.87d + 0.19r + 0.11\alpha$
(ν_1)	606	613	613	$0.80r + 0.10d$
(ν_{4a})	362	378	378	$1.03\alpha + 0.35s + 0.30\varphi$
	289	291	unobs.	0.69φ
	199	180	unobs. (<250)	$0.59s + 0.54\varphi + 0.37\alpha$
B_1 (ν_{3a})	894	893	893	0.92d
(ν_{4c})	320	304	304	$0.79\varphi + 0.16w$
	102	102	unobs. (<250)	$0.83w + 0.14\varphi$
B_2 (ν_{3c})	674	669	669	$0.87r + 0.18\varphi$
(ν_{4b})	229	339	339	$0.61\varphi + 0.12s + 0.12r$
	299	200	unobs. (<250)	$0.91s + 0.25\varphi$
		$LiAlF_4$		
A_1 (ν_{3b})	818	817	817	$0.90d + 0.17r + 0.13\alpha$
(ν_1)	601	608	608	0.92r
(ν_{4a})	557	560	560	1.26s
	360	361	unobs.	1.27α
	270	220	220	$1.35\varphi + 0.22\alpha$
B_1 (ν_{3a})	903	911	911	0.92d
(ν_{4c})	328	316	316	$0.71\varphi + 0.24w$
	158	157	unobs. (<250)	$0.76w + 0.22\varphi$
B_2 (ν_{3c})	654	644	644	$0.76r + 0.15\varphi$
(ν_{4b})	451	450	450	0.95s
	286	270	270	$0.84\varphi + 0.18r$

[a] Estimated gas-phase frequencies [11].
[b] Terms below 0.1 are omitted.

An adjustment of the symmetry force constants to fit the observed frequencies for the $AlkAlF_4$ molecules (keeping the L-matrix constant) had only a minor influence on the matrices. Table 9 gives the

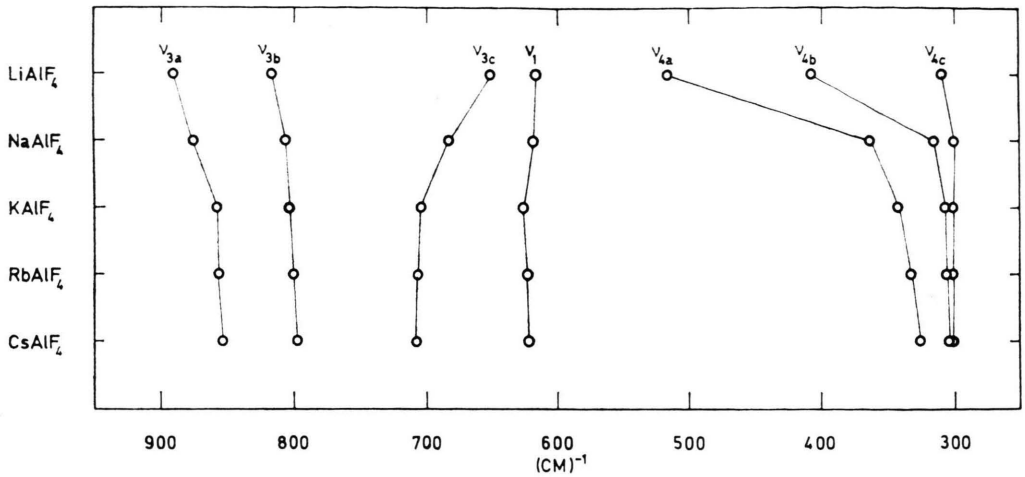

Fig. 7. Correlation diagram of observed frequencies of the $AlkAlF_4$ molecules isolated in argon matrices.

resulting symmetrized matrices for $LiAlF_4$ which are considered as the final force field. Complete sets of calculated frequencies for the five molecules from the final force fields are included in Table 8, as well as potential energy distribution (PED). The PED terms have been calculated utilizing diagonal terms only, according to:

$$X_{ik} = F_{ii} L_{ik}^2 / \lambda_k .$$

Frequencies that are unobserved, have been taken from the approximate calculations, with some exceptions. As noted earlier, two bands at 268 and 221 cm^{-1} were found for $^7LiAlF_4$ in neon [10] that had no counterparts in the other spectra. Now, computations show these modes to be at higher frequencies than observed. Accordingly in the final force field calculations, the lowest A_1 and B_2 frequencies have been set to 220 and 270 cm^{-1}, respectively, for $LiAlF_4$. A similar adjustment has also been performed with $NaAlF_4$ (and to a minor degree with $KAlF_4$). This procedure influences the F_{55} symmetry force constant of A_1 and the F_{33} of B_2 (cf. Table 9). The largest difference between calculated and observed frequencies has been found for the frequencies assigned to bending modes (cf. Table 7). It was found very difficult to select suitable bending force constants that gave a better fit to the observed frequencies. Furthermore, from the PED it is seen that the bending frequencies to some extent are influenced by the other strong stretching force constants. For this reason, few attempts were made to refine the approximated bending force constants any further.

Table 9. Final symmetry force constants (mdyne/Å) for $LiAlF_4$ with symmetry C_{2v}. Species A_2 omitted.

Species A_1					
3.621					
−0.778	1.632				
0.637	0.003	4.806			
0.474	−0.494	0.004	0.904		
−0.039	−0.062	0.036	0.479	0.964	
Species B_1			Species B_2		
4.445			1.963		
−0.023	0.256		0.040	0.505	
−0.007	−0.004	0.097	−0.022	−0.000	0.244

Matrix Shifts and Vibrational Interactions of the Alkali Atoms

Figure 7 gives a survey of the frequencies observed for the $AlkAlF_4$ molecules in argon matrices. The variation of the nitrogen frequencies with the alkali atoms is similar. The observation that the three ν_3-frequencies are seen to split the most with lithium as counteratom, is in accordance with the expected influence of the polarizing power of the alkali atoms, which increases when going from Cs to Li. The greater the polarizing power of the counteratom, the more it weakens the neighbouring $Al\text{-}F_b$ bridge bond and decreases the stretching frequencies associated with these two bonds. Due to the weakening of the $Al\text{-}F_b$ bond, it is not unreasonable to infer that the $Al\text{-}F_t$ terminal bond should be strengthened, resulting in an increase of the frequencies associated with these bonds. This reasoning is illustrated by the PED for $AlkAlF_4$ in

Table 8. The two highest Al-F stretching frequencies $\nu_{3b}(A_1)$ and $\nu_{3a}(B_1)$, which show a general increase from $CsAlF_4$ to $LiAlF_4$, are associated with mainly Al-$F_t(d)$ stretching modes, while the two lowest Al-F stretching frequencies $\nu_{3c}(B_2)$ and $\nu_1(A_1)$, which show a general decrease when going from $CsAlF_4$ to $LiAlF_4$, are largely related to Al-F_b(r) stretching modes. Notably, the ν_{3a} and ν_{3c} frequencies have generally quite different shifts between argon and nitrogen (viz. Table 3). The ν_{3a} frequencies experience a red shift (average value of $-9\ cm^{-1}$) from argon to nitrogen, while the ν_{3c} frequencies are drastically blueshifted (average value of $+22\ cm^{-1}$). Usually, antisymmetric stretching frequencies show red shifts [34, 35, 36].

These matrix shifts support the results from the PED showing the ν_{3a} and the ν_{3c} frequencies to be related to different vibrational stretching modes. Matrix shifts may be interpreted in terms of the "tight cage" and "loose cage" terminology of Pimentel and Charles [34] (see also [36] for discussion). Weak force constant coordinates are more likely to be in a "tight cage" environment than coordinates associated with strong force constants. Fundamentals related to strong force constants are observed to display negative shifts (relative to the gas-phase value), while low-frequency stretching as well as bending or rocking vibrations give positive shifts.

The frequency shifts between argon and nitrogen for ν_{4a} and ν_{4b} are seen to decrease from $LiAlF_4$ to $CsAlF_4$, viz., from a large red shift for $LiAlF_4$ (-40 and $-31\ cm^{-1}$) to a small shift for $CsAlF_4$ (-3 and $-1\ cm^{-1}$). These shifts seem to indicate that the fundamental vibrations responsible for the ν_{4a} and ν_{4b} frequencies are different in $LiAlF_4$ and $CsAlF_4$, and that there is a mixture of fundamentals in these two frequencies for the three other molecules (cf. Tables 3 and 8).

Brooker and Bredig [37] have shown the vibrational frequencies of the NO_3^- entity in matrix isolated MNO_3 (M = Li, Na, K, Rb, Th(I) and Cu(II) to correlate with the effective polarizing power of the cation M^+. Janz and James [38] defining polarizing power as the product of the effective polarizing power S_{eff} and z/r, found good correlation between the polarizing power so defined and the Raman frequency of the ν_1 symmetric stretch of molten nitrate melts.

The presently obtained frequencies gives the best correlation when the polarizing power defined by Janz and James [38] is used (Figure 8). Anyhow, it appears that the polarizing power of the alkali metals is a dominant cause of the distortion of the $AlkAlF_4$ molecules.

Rytter and Øye [39] and Rytter [40] observed a regular increase of the $\nu_3(F_2)$ stretching frequency of $AlCl_4^-$ when going from Cs to Li. This increase was explained by a mass effect which may be described in terms of quasi-lattice interactions. In order to investigate the influence of the change of mass of the alkali atoms, the final force fields for $CsAlF_4$ and $LiAlF_4$ were used, only varying the mass of the alkali atom and the Alk-F_b length. It was confirmed in the computations that the observed variation of the Al-F stretching frequencies cannot be explained by a mass effect, but is described by the change of the Al-F valence force constants as shown in Table 7.

The interaction of the alkali cations with molten aluminium tetrachloride mixtures is much weaker, and probably significantly different, from the

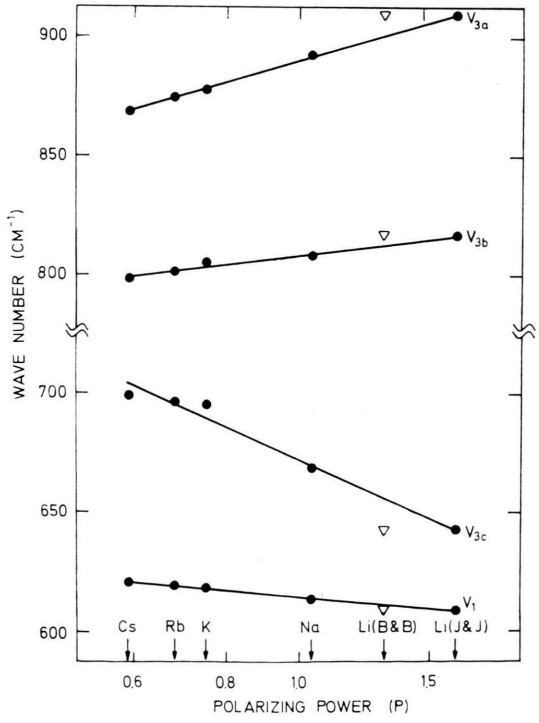

Fig. 8. Estimated gas-phase frequencies as a function of the polarizing power of the alkali atoms. Filled circles: $P = (z/r)\,S_{eff}$ according to Janz and James [38]. Triangles: $P = z/(rS_{eff})$ according to Brooker and Bredig [37].

Table 10. Comparison of frequency shifts (cm^{-1}) between argon and nitrogen matrices ($\nu_{Ar}-\nu_{N_2}$) with percent contribution from Alk-F stretching of the PED for the ν_{4a} and ν_{4b} frequencies. % Alk-F stretching is calculated from the complete PED.

Molecule	ν_{4a}		ν_{4b}	
	$\nu_{Ar}-\nu_{N_2}$	% Alk-F stretching	$\nu_{Ar}-\nu_{N_2}$	% Alk-F stretching
$CsAlF_4$	− 3	5.6	− 1	4.5
$RbAlF_4$	− 9	6.8	− 2	4.9
$KAlF_4$	−10	10.6	− 4	7.3
$NaAlF_4$	−16	20.8	− 6	14.2
$LiAlF_4$	−40	86.6	−31	93.6

interaction in gaseous alkali tetrafluoroaluminates. This is most evident from the large splitting of the ν_3 frequencies of the $AlkAlF_4$ molecules. On the other hand, Rytter et al. [41] explained the observed splitting of the ν_3-frequency of molten $Li^+AlCl_4^-$ in terms of a structural entity with symmetry C_{2v}. A reduction of the Al-Cl_b and an increase of the Al-Cl_t force constants satisfactorily accounted for the observed splitting. This is in agreement with the explanation given for the splitting of the ν_3-frequencies of $AlkAlF_4$ in this work.

A comparison of the PED and the frequency shifts between argon and nitrogen matrices for the ν_{4a} and ν_{4b} frequencies (cf. Tables 3 and 8) reveals interesting qualitative features. This is illustrated in Table 10. The percentage of Alk-F stretching contribution in these two frequencies from the PED relates to the magnitude of the observed shifts. The large shifts observed with $LiAlF_4$ are in accordance with the large shift ($\sim 60\ cm^{-1}$) observed for LiF between argon and nitrogen [42]. It looks like symmetric Alk-F stretching is related to larger frequency shifts than the antisymmetric stretching mode.

Isotopic Shifts

In order to test the new assignments of frequencies for the $AlkAlF_4$ molecules, approximate computations were performed using the force field for $LiAlF_4$ (cf. Tables 7 and 8) only substituting with ^7Li and ^6Li. The results of these computations are shown in Table 11. Also listed in Table 11, are calculated frequencies for $^6LiAlF_4$ based on a force field fitted to the observed frequencies of $^7LiAlF_4$ in neon matrix. For comparison, the observed frequencies for $^6LiAlF_4$ and $^7LiAlF_4$ are shown. Isotopic shifts ($\Delta = \nu(^6Li) - \nu(^7Li)$) are indicated.

The very good agreement between the observed and calculated isotopic shifts (largest difference: $8\ cm^{-1}$) confirms the proposed frequency assignment of Table 9. It is also noteable that the isotopic shifts for LiF symmetric and antisymmetric stretch are observed to be 41 and 22 cm^{-1}, respectively, for matrix isolated $LiBeF_3$ [21]. These are very close to the corresponding isotopic shifts observed for $LiAlF_4$.

The Molecular Structure in the Vapour Phase

Finally, it should be mentioned that the observation of four frequencies in the high frequency region ($600-900\ cm^{-1}$) is not a definite confirmation of a true bidentate structure with symmetry C_{2v} [26].

An electron diffraction investigation has been performed on the vapour phase molecular structure of $KAlF_4(g)$ [43]. The sample used in the electron diffraction experiments was from the same batch as used in this study [11]. In general, the results from the electron diffraction work is in good agreement with our interpretation of the spectroscopic data. Specifically, it is agreed that the alkali metal-fluorine bond is a rather weak bond and the

Table 11. Calculated and observed isotopic frequency shifts (cm^{-1}) for $^6LiAlF_4$ and $^7LiAlF_4$. $\Delta = \nu(^6Li)-\nu(^7Li)$.

Species	Approximate force fields			Final force field based on neon frequencies for $^7LiAlF_4$			Observed		
	^6Li	^7Li	Δ	^6Li	^7Li	Δ	^6Li	^7Li	Δ
A_1	818	818	0	817	817	0	901	900	1
	606	601	5	614	611	3	(611)	(611)	0
	584	555	29	571	541	30	577	541	36
	363	360	3	364	361	3			
	271	270	1	222	221	1	222	221	1
B_1	903	903	0	900	900	0	818	817	1
	330	328	2	315	313	2	316	313	3
	167	158	9	166	157	0			
B_2	655	654	1	651	649	2	651	649	2
	477	449	28	460	433	27	453	433	20
	286	286	0	268	268	0	269	268	1

Al-F_t bond is stronger than the corresponding Al-F_b bond, the interatomic distances being equal or nearly equal.

In fitting the electron diffraction data to a static model [43], best approximation was found for Model II, (Fig. 6) with a puckered four-membered ring having C_s-symmetry. It was very difficult to determine the exact position of the potassium atom, and none of the three other models considered could be excluded.

Rambidi [44] has suggested from electrostatic considerations that at high temperatures the alkali atom may move on a surface circumscribed about the AlF_4^- entity. However, a minimum was found for the potential energy when the alkali atom was in a position normal to the tetrahedron edge (symmetry C_{2v}). At low temperatures, like in a matrix isolation experiment, he claims that the internuclear distances is close to the rigid equilibrium configuration of the molecule. Hence, the recorded spectra probably are interpreted best in terms of a C_{2v} symmetry model.

Acknowledgement

This work has been supported by *Anders Jahres Fond til Vitenskapens fremme* and *Elektrokemisk Forskningsfond, Elkem-Spigerverket A/S* and *Norges Tekniske Naturvitenskapelige Forskningsråd.* Useful discussion with Dr. E. Rytter is gratefully acknowledged.

[1] J. P. Devlin, in: Advances of Infrared and Raman Spectroscopy, R. J. H. Clark and R. E. Hester, Eds., **2**, 153 (1976).
[2] C. N. Cockran, Trans. Met. Soc. AIME **239**, 1056 (1967).
[3] A. Büchler and J. B. Berkowitz-Mattuck, in: L. Eyring, Ed., Advances in High-Temperature Chemistry, Academic Press, New York 1967, Vol. 1, p. 133.
[4] L. N. Sidorov, E. N. Kolosov, and V. B. Shol'ts, Russ. J. Phys. Chem. **42**, 1382 (1968).
[5] V. B. Shol'ts and L. N. Sidorov, Vestn. Mosk. Univ. Khim. **4**, 371 (1972).
[6] R. F. Porter and E. E. Zeller, J. Chem. Phys. **33**, 858 (1960).
[7] L. N. Sidorov and N. A. Zhegulskaya, Int. J. Mass Spectr. Ion Phys. **17**, 111 (1975).
[8] L. D. McCory, R. C. Paule, and J. L. Margrave, J. Phys. Chem. **67**, 1086 (1963).
[9] V. P. Spiridonov and E. V. Erokhin, Zh. Neorg. Khim. **14**, 636 (1969).
[10] S. J. Cyvin, B. N. Cyvin, and A. Snelson, J. Phys. Chem. **75**, 2609 (1971).
[11] R. Huglen, Thesis No. 32, Institutt for Uorganisk kjemi, Norges Tekniske Høgskole, Universitetet i Trondheim, Norway, 1976.
[12] S. J. Cyvin, B. N. Cyvin, and A. Snelson, J. Phys. Chem. **74**, 4338 (1970).
[13] A. Snelson, J. Chem. Phys. **46**, 3652 (1967).
[14] S. J. Cyvin, B. N. Cyvin, D. B. Rao, and A. Snelson, Z. anorg. allg. Chem. **380**, 212 (1971).
[15] H. Hovdan, R. Huglen, and H. A. Øye, Proceedings of the Fourth Nordic High Temperature Symposium-Nortemps-75, 1975, Vol. 1, p. 107.
[16] V. P. Spiridonov, E. V. Erokhin, and B. I. Lutoshkin, Vestn. Mosk. Univ. Khim. **12**, 296 (1971).
[17] V. P. Spiridonov, Yu. A. Brezgin, and M. I. Shakhparonov, Zh. Strukt. Khim. **12**, 1080 (1971).
[18] V. P. Spiridonov, Yu. A. Brezgin, and M. I. Shakhparanov, Zh. Strukt. Khim. **13**, 321 (1972).
[19] V. P. Spiridonov, A. N. Khodchenkov, and P. A. Akishin, Vestn. Mosk. Univ. Khim. **6**, 34 (1965).
[20] N. M. Roddatis, S. M. Tolmachev, V. V. Ugarov, and N. G. Rambidi, Zh. Strukt. Khim. **15**, 693 (1974).
[21] A. Snelson, B. N. Cyvin, and S. J. Cyvin, J. Mol. Struct. **24**, 165 (1975).
[22] B. Gilbert, G. Mamantov, and G. M. Begun, Inorg. Nucl. Chem. Letters **10**, 1123 (1974).
[23] C. Solomons, J. H. R. Clarke, and O'M. Bockris, J. Chem. Phys. **49**, 445 (1968).
[24] S. K. Ratkje and E. Rytter, J. Phys. Chem. **78**, 1499 (1974).
[25] E. Rytter and S. K. Ratkje, Acta Chem. Scand. **A 29**, 565 (1975).
[26] G. Ritzhaupt and J. P. Devlin, J. Chem. Phys. **62**, 1982 (1975).
[27] A. Müller, J. Phys. Chem. Leipzig **238**, 116 (1968).
[28] A. Müller, C. J. Peacock, H. Schultze, and U. Heidborn, J. Mol. Structure **3**, 252 (1969).
[29] K. Nakamoto, Infrared Spectra of inorganic and coordination compounds, 2. ed., Wiley Interscience, New York 1970.
[30] S. J. Cyvin, Molecular Vibrations and Mean Square Amplitudes, Universitetsforlaget, Oslo and Elsevier, Amsterdam 1968.
[31] S. J. Cyvin, Ed., Molecular Structures and Vibrations, Elsevier, Amsterdam 1972.
[32] S. J. Cyvin and B. N. Cyvin, Acta Chem. Scand. **23**, 3139 (1969).
[33] B. N. Cyvin and S. J. Cyvin, J. Mol. Structure **24**, 177 (1975).
[34] G. C. Pimentel and S. W. Charles, Pure Appl. Chem. **7**, 111 (1963).
[35] W. Hastie, R. H. Hauge, and J. L. Margrave, in: C. N. R. Rao and J. R. Ferraro, Eds., Spectroscopy in Inorganic Chemistry, Vol. 1, Academic Press, New York 1973.
[36] A. J. Barnes, in: H. E. Hallam, Ed., Vibrational Spectroscopy of Trapped Species, chap. 4, John Wiley & Sons, London 1973.
[37] M. H. Brooker and M. A. Bredig, J. Chem. Phys. **58**, 5319 (1973).
[38] G. J. Janz and D. W. James, J. Chem. Phys. **36**, 739 (1961).
[39] E. Rytter and H. A. Øye, J. Inorg. Nucl. Chem. **35**, 4311 (1973).
[40] E. Rytter, Thesis No. 26, Institutt for Uorganisk Kjemi, Norges Tekniske Høgskole, Universitetet i Trondheim, Norway 1974.
[41] E. Rytter, H. A. Øye, S. J. Cyvin, B. N. Cyvin, and P. Klaeboe, J. Inorg. Nucl. Chem. **35**, 1185 (1973).
[42] M. J. Linevsky, J. Chem. Phys. **34**, 587 (1961).
[43] E. Vajda, I. Hargittai, and J. Tremmel, Inorg. Chim. Acta **25**, 143 (1977).
[44] N. G. Rambidi, J. Mol. Structure **28**, 77 and 89 (1975).